

1 **Widespread microbial mercury methylation genes in the global ocean**

2 Emilie Villar<sup>1,2</sup>, Lea Cabrol<sup>1\*</sup>, Lars-Eric Heimbürger-Boavida<sup>1\*</sup>

3

4 <sup>1</sup>Aix Marseille Université, Univ Toulon, CNRS, IRD, Mediterranean Institute of Oceanography  
5 (MIO) UM 110, 13288, Marseille, France

6 <sup>2</sup>Sorbonne Université, Université Pierre et Marie Curie - Paris 6, CNRS, UMR 7144 (AD2M),  
7 Station Biologique de Roscoff, Place Georges Teissier, CS90074, Roscoff, 29688 France

8 \*Both authors contributed equally to this work.

9 Corresponding Author: Léa Cabrol, [lea.cabrol@mio.osupytheas.fr](mailto:lea.cabrol@mio.osupytheas.fr)

10

11 **Abstract**

12 Methylmercury is a neurotoxin that bioaccumulates from seawater to high concentrations in  
13 marine fish, putting human and ecosystem health at risk. High methylmercury levels have  
14 been found in the oxic subsurface waters of all oceans, yet only anaerobic microorganisms  
15 have been identified so far as efficient methylmercury producers in anoxic environments.  
16 The microaerophilic nitrite oxidizing bacteria *Nitrospina* has been previously suggested as a  
17 possible mercury methylator in Antarctic sea ice. However, the microorganisms processing  
18 inorganic mercury into methylmercury in oxic seawater remain unknown. Here we show  
19 metagenomic evidence from open ocean for widespread microbial methylmercury  
20 production in oxic subsurface waters. We find high abundances of the key mercury  
21 methylating genes *hgcAB* across all oceans corresponding to taxonomic relatives of known  
22 mercury methylators from Deltaproteobacteria, Firmicutes and Chloroflexi. Our results

23 identify *Nitrospina* as the predominant and widespread key player for methylmercury  
24 production in the oxic subsurface waters of the global ocean.

25

## 26 **Introduction**

27 Human activities release 2500 tons of inorganic mercury (Hg) every year and have added 55  
28 000 tons of Hg to the global ocean since the industrial revolution <sup>1</sup>. Humans are exposed to  
29 Hg in the form of methylmercury (MeHg), mainly through the consumption of marine fish.  
30 The Minamata Convention ([www.mercuryconvention.org](http://www.mercuryconvention.org)) aims to protect human health  
31 from the adverse effects of Hg *via* the reduction of anthropogenic, inorganic Hg emissions.  
32 To understand the efficacy and time-scales of lowered Hg emissions to reduce fish MeHg  
33 levels, we must fully understand the origin of marine MeHg. Microorganisms play a central  
34 role in Hg transformations. We must identify the Hg methylating microbes and the factors  
35 controlling their distribution in order to better constrain MeHg production in the global  
36 ocean.

37 As the only cultured microbes known to produce MeHg to date are anaerobic, research  
38 focused for many years on a MeHg source in anoxic marine sediments <sup>2-5</sup>. However, several  
39 lines of independent evidence speak in favour of *in situ* MeHg production in oxic seawater as  
40 the main source of fish MeHg. Recent large scale oceanographic expeditions found  
41 subsurface MeHg maxima in every ocean basin <sup>4,6</sup>. The proportion of MeHg to inorganic Hg  
42 throughout the oxic seawater column is higher than those found in anoxic sediments.

43 Laboratory experiments show that Hg methylation can occur in anaerobic microniches that  
44 occur within sinking particles in oxic waters <sup>7</sup>. Bianchi et al. <sup>8</sup> provide compelling evidence  
45 that anaerobic microbes thrive in anoxic microenvironments of sinking particulate organic  
46 matter. Independently, incubation experiments with isotopically labelled Hg spikes show

47 significant *in situ* Hg methylation in oxic seawater<sup>9</sup>. Additional evidence stems from Hg  
48 stable isotope signatures of marine fish, that can only be explained if 60-80% of the MeHg is  
49 produced in open ocean subsurface waters<sup>10</sup>. Lastly, a pioneering study found a compound  
50 specific  $\delta^{13}\text{C}$  signature of fish tissue MeHg similar to algal  $\delta^{13}\text{C}$ , suggesting that MeHg is  
51 produced in the open ocean water column<sup>11</sup>.

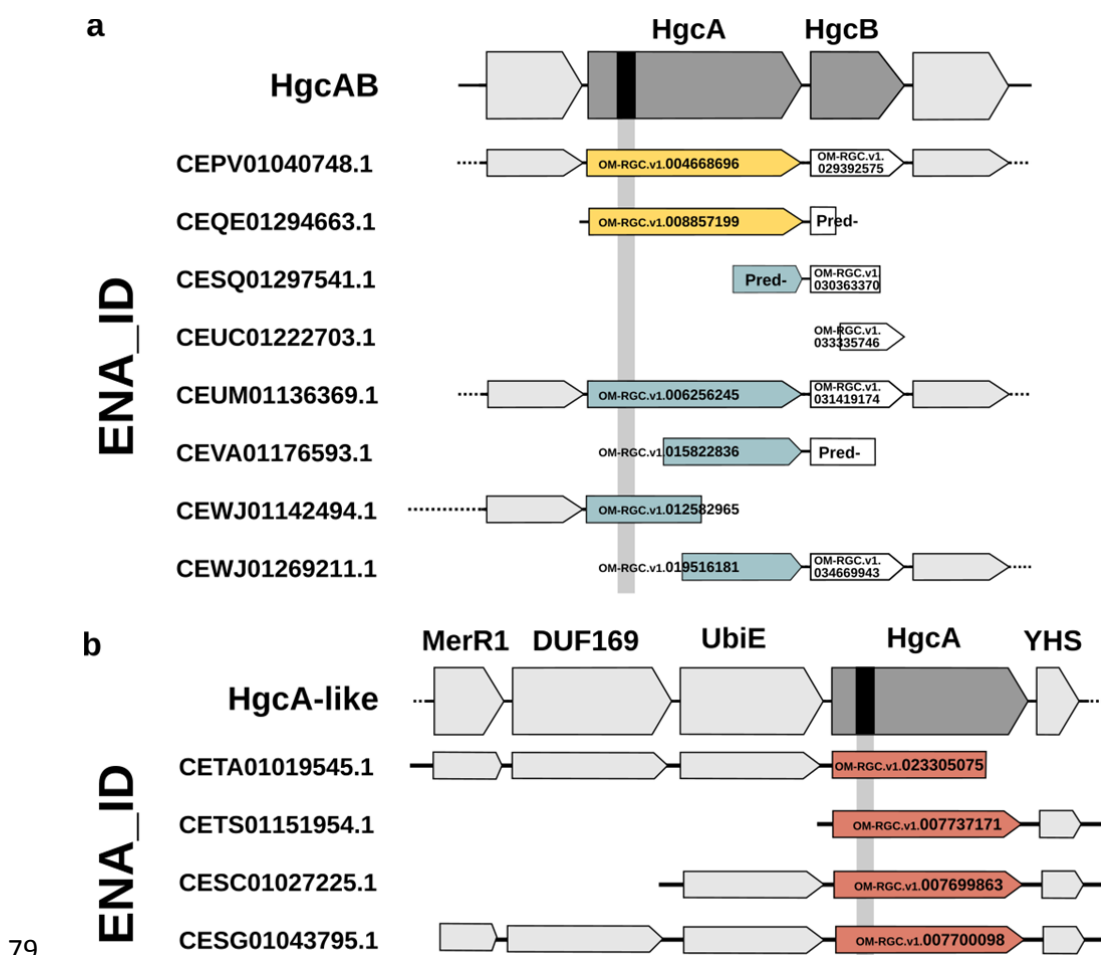
52 A major breakthrough has been made with the discovery of two key genes, *hgcA* and *hgcB*,  
53 that control Hg methylation in model anaerobic Hg-methylators<sup>5</sup>. The presence of the *hgcAB*  
54 operon predicts Hg methylation capacity in diverse microorganisms<sup>2</sup>. A screening of publicly  
55 available microbial metagenomes found the *hgcAB* genes in nearly all anaerobic  
56 environments, but the study only rarely detected the genes in pelagic marine water column  
57 metagenomes in the open ocean<sup>12</sup>. In antarctic sea ice a marine microaerophilic nitrite  
58 oxidizing bacterium belonging to the *Nitrospina* genus has been recently identified as a  
59 potential Hg methylator with HgcA-like proteins<sup>13</sup>. We aim to resolve the paradox between  
60 the wealth of geochemical evidence for *in situ* MeHg production and the absence of known  
61 anaerobic Hg methylators in the open ocean. Metagenomic data from 243 *Tara* Oceans  
62 samples from 68 open ocean locations covering most ocean basins was analysed to generate  
63 an ocean microbial reference gene catalog<sup>14</sup>. We screened the *Tara* Oceans metagenomes  
64 for the presence of the key *hgcA* methylating gene and provide compelling evidence on the  
65 potential key players producing MeHg in the open ocean.

66 Results and Discussion

### 67 **Identification of HgcAB homologs in the ocean gene catalog**

68 Ten *hgcA* and 5 *hgcB* homolog genes were identified in the Ocean Microbial Reference Gene  
69 Catalog<sup>14</sup> (OM-RGC), 6 scaffolds presenting simultaneously *hgcA* and *hgcB* (Fig. 1,

70 Supplementary Table 1). Alignment of HgcA sequences revealed 7 sequences with the  
 71 conserved NVWCAA motif<sup>5</sup> and one sequence with the modified NIWCAA motif on the ‘cap  
 72 helix’ region. Mutation experiments previously showed that the structure of the putative  
 73 ‘cap helix’ region harbouring Cys93 is crucial for methylation function<sup>15</sup>. Two HgcA  
 74 sequences were truncated (OM-RGC.v1.019516181, OM-RGC.v1.015822836), preventing  
 75 inspection of their conserved motif, but they could be unequivocally assigned to HgcA  
 76 sequences based on their phylogenetic placement and high similarity with known HgcA  
 77 sequences (Fig. 2). The 5 HgcB sequences presented the conserved motif ECGAC<sup>5</sup>  
 78 (Supplementary Table 1).



79  
 80 **Figure 1 | The genomic context of the HgcA orthologs. a, HgcAB operon. b, HgcA-like proteins. The**  
 81 12 retrieved scaffigs are identified by their ENA\_ID on the left of the figure. The solid lines represent

82 the extent of the scaftig sequence and the dashed lines indicate that the scaftig sequence is longer  
83 than the represented part. The location of the conserved motif is indicated on the HgcA box by a  
84 black bar. When present in *Tara* Oceans samples, the corresponding gene identifier is indicated on  
85 the bar for HgcA and HgcB, or indicated as (Pred-) if the gene was incomplete and the protein  
86 sequence was partially predicted. The colour of the HgcA boxes refers to the biogeographical  
87 clustering as defined in Fig.3 (Cluster 1 in blue, Cluster 2 in yellow, Cluster 3 in red). For Cluster 3  
88 sequences (assigned to *Nitrospina*), the genomic context was enlarged to show the closest sequences  
89 (MerR1: mercuric resistance operon regulatory protein, UbiE: Ubiquinone/menaquinone  
90 biosynthesis C-methyltransferase, DUF169: Hypothetical protein with DUF 169 motif, YHS:  
91 Hypothetical protein with YHS domain).

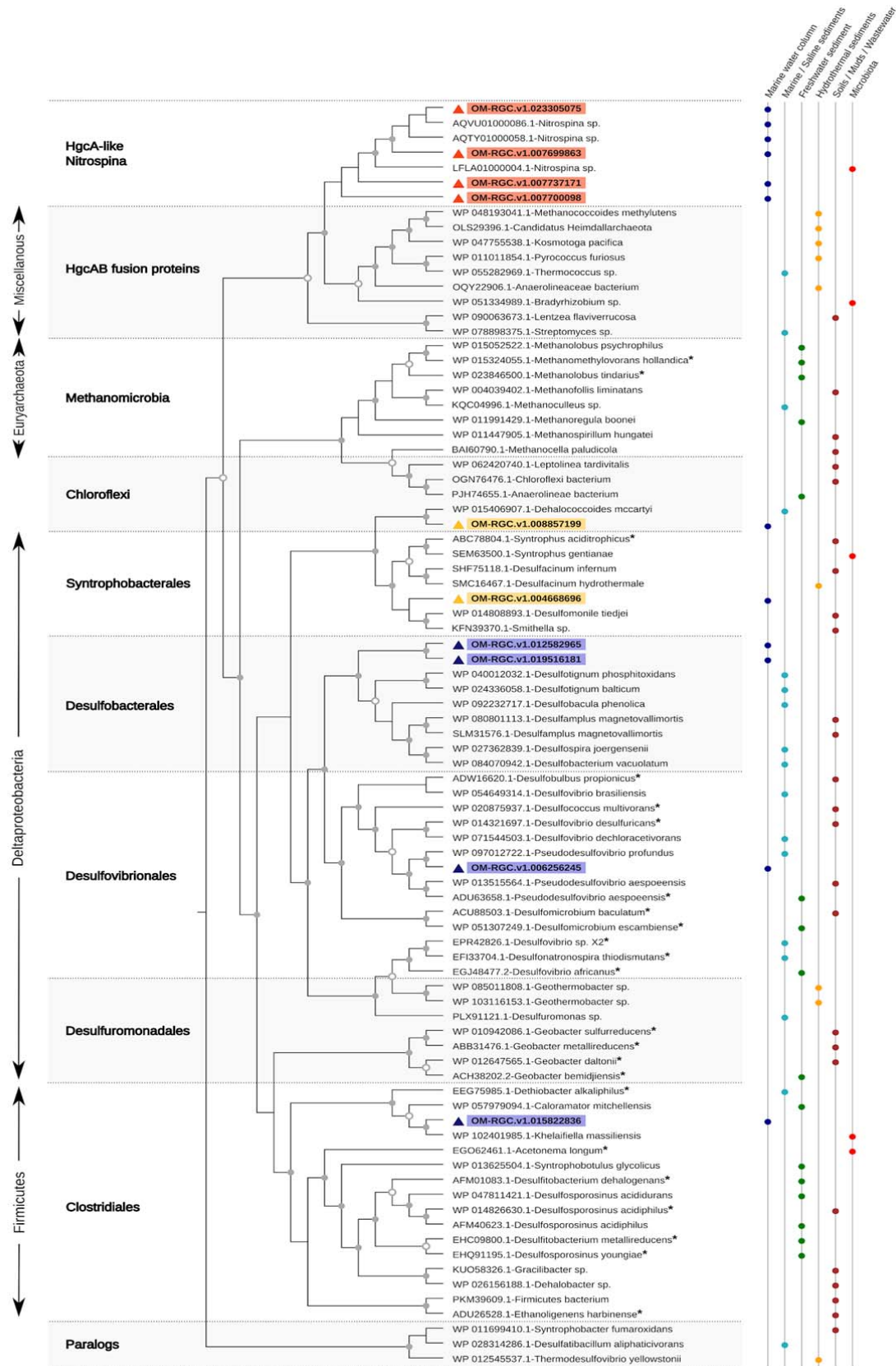
92

### 93 **HgcA sequences found in the Tara Oceans assemblies covered nearly all known Hg** 94 **methylators**

95 Phylogenetic placement of the 10 sequences found in the *Tara* Oceans assemblies covered  
96 nearly all known Hg methylators (Fig. 2). Four sequences (OM-RGC.v1.007700098, OM-  
97 RGC.v1.007737171, OM-RGC.v1.023305075, OM-RGC.v1.007699863) were closely related to  
98 the HgcA-like proteins described by Gionfriddo et al.<sup>13</sup> for *Nitrospina* sp. The *Nitrospinae*  
99 phylum has been described as a distinct phylogenetic group of lithoautotrophic nitrite  
100 oxidizing bacteria exclusively found in marine environments<sup>16</sup>, particularly abundant in  
101 oxygen-deficient zones<sup>17</sup>.

102 The remaining 6 HgcA sequences were distributed between Deltaproteobacteria, Firmicutes  
103 and Chloroflexi phyla. Within Deltaproteobacteria, three orders were represented, namely  
104 *Desulfovibrionales*, *Desulfobacterales* and *Syntrophobacterales*. OM-RGC.v1.006256245 was  
105 most closely related to HgcA from *Pseudodesulfovibrio profundus*, a strictly anaerobic  
106 piezophilic sulfate-reducer bacteria (SRB) previously isolated from marine sediment<sup>18</sup>. It  
107 belongs to the *Desulfovibrionales* order, which contains several members with confirmed  
108 Hg-methylating capacity, such as the model species *Desulfovibrio desulfuricans* with

109 exceptionally high Hg-methylation rates, isolated from estuarine sediments<sup>19</sup>. OM-  
110 RGC.v1.019516181 and OM-RGC.v1.012582965 belonged to *Desulfobacterales*, a well-known  
111 order of SRB containing efficient Hg-methylators such as *Desulfobulbus propionicus* and  
112 *Desulfococcus multivorans*. Finally, OM-RGC.v1.004668696 belonged to  
113 Syntrophobacterales. The closest relative of OM-RGC.v1.004668696 with strong confirmed  
114 methylation potential was the non-SRB obligate syntroph *Syntrophus aciditrophicus*<sup>2</sup>.  
115 Syntrophic bacteria are important Hg-methylators in low-sulfate ecosystems<sup>20,21</sup>, where  
116 they degrade OM in association with H<sub>2</sub>-consuming microorganisms such as sulfate-  
117 reducers, iron-reducers and methanogens.  
118 Within Firmicutes, OM-RGC.v1.015822836 was tightly related to HgcA from recently isolated  
119 human gut bacteria *Khelaifiella* in the Clostridiales order<sup>22</sup>. Their closest relative with  
120 confirmed methylation potential is the non-SRB *Dethiobacter alkaliphilus*, with low to  
121 moderate Hg-methylation capacity<sup>2</sup>.  
122 OM-RGC.v1.008857199 was related to Chloroflexi, a phylum for which several *hgcAB*-  
123 carriers have been identified, but for which experimental confirmation of Hg methylation  
124 capacity is still needed. This sequence clusters tightly with HgcA from *Dehalococcoides*  
125 *mccartyi*, which has been reported as a potential methylator, albeit in minor abundance, in  
126 freshwater marshes<sup>20</sup>. These two sequences are separated from other Chloroflexi HgcA  
127 sequences and more closely related to HgcA sequences from Syntrophobacterales, showing  
128 that the taxonomy and the HgcA-phylogeny are not always congruent. The phylogenetically  
129 irregular distribution of *hgcA* can be an indication of horizontal gene transfers (HGT) and/or  
130 gene deletions in response to stress, suggesting the prevalent influence of environment on  
131 Hg-methylation ability<sup>23</sup>.





133 **Figure 2 | Phylogenetic tree of HgcA homolog sequences found in the *Tara* Oceans assemblies**

134 Maximum likelihood phylogenies were inferred using PhyML Best AIC Tree with the best model of  
135 sequence evolution Blosum62+I+G+F. Branch support was calculated using the non-parametric  
136 Shimodaira-Hasegawa-like approximate likelihood ratio test. The triangle colour refers to the  
137 biogeographical clustering of the HgcA sequences retrieved from *Tara* Oceans assemblies, as defined  
138 in Fig.3 (Cluster 1 in blue, Cluster 2 in yellow, Cluster 3 in red). The tree was rooted using 3  
139 paralogues from confirmed non-Hg methylating bacteria. Sequences from experimentally confirmed  
140 mercury methylators were indicated with an asterisk. Support values using 1,000 resamples are  
141 shown when >50 and coloured squares indicate the isolation source.

142

143 Among the 10 HgcA sequences found in the gene ocean catalogue, none was affiliated to  
144 methanogenic *Archaea*. Even if the co-existence of methanogens and sulfate-reducers has  
145 been evidenced in marine sediments<sup>24</sup>, sulfate reduction usually outcompetes  
146 methanogenesis in seawater under non-limiting sulfate concentrations<sup>25</sup>. Our results thus  
147 show that Hg-methylators in the ocean span a large taxonomic diversity, not limited to  
148 sulfate-reducing bacteria.

149

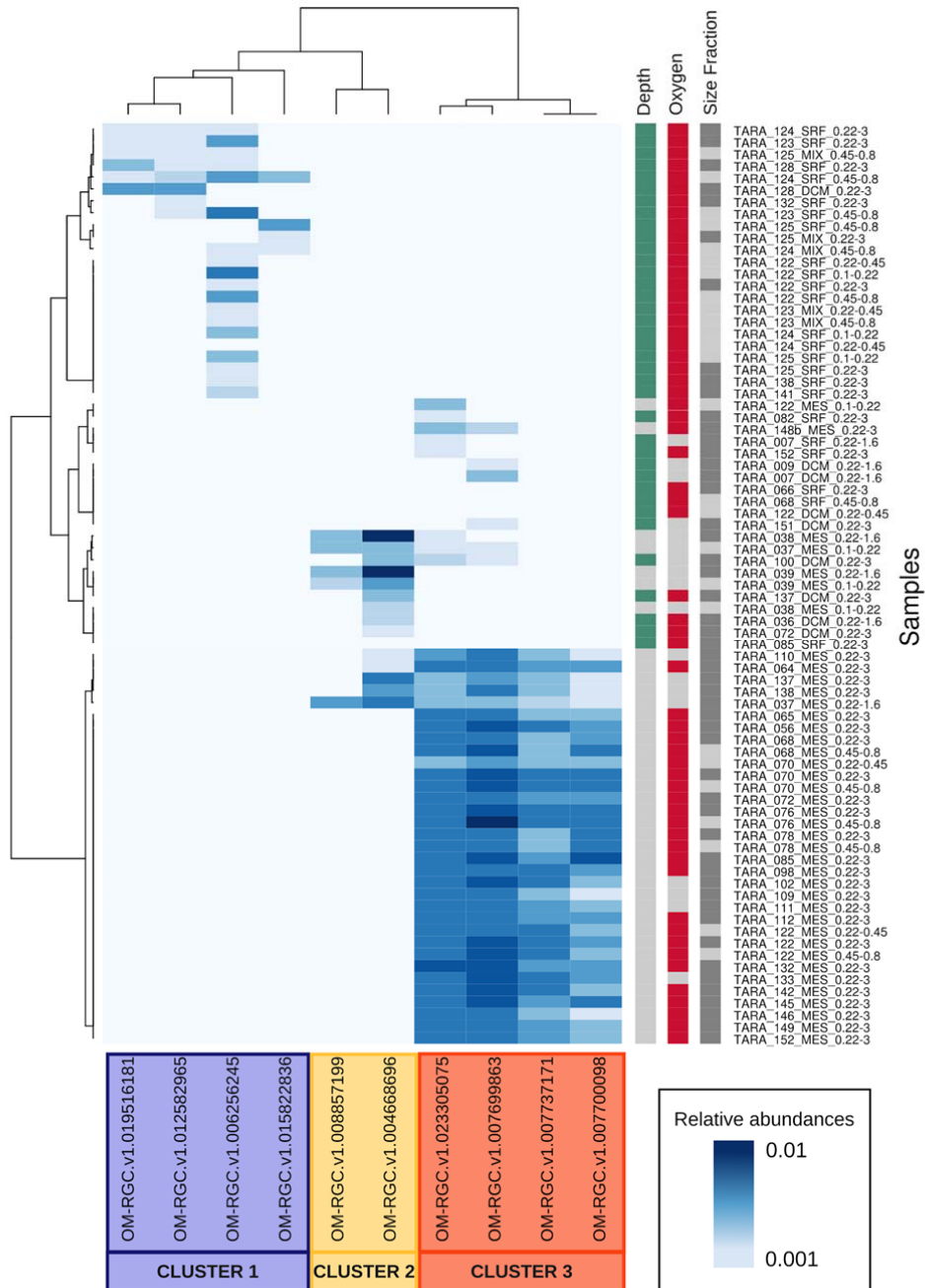
150 **Biogeography distinguishes three groups of putative marine Hg methylators**

151 Once clearly identified and phylogenetically assigned, the biogeographic distribution  
152 patterns of *hgcA* was evaluated. The 10 HgcA sequences were identified in 77 samples out  
153 of the 243 available *Tara* Oceans metagenomes and were clearly distributed in three clusters  
154 according to their abundance patterns (Fig. 3). The biogeographic clustering was consistent  
155 with the HgcA-phylogeny.

156 Cluster 1 gathered Desulfobacterales, Clostridiales and Desulfovibrionales HgcA sequences,  
157 exclusively present in 23 oxic surface waters (< 120 m-depth, > 10  $\mu\text{M}_{\text{O}_2}$ ). Highest  
158 abundances were found in the photic zone of the Pacific Ocean, especially in the area  
159 surrounding the Marquesas Islands. This region is characterized by extensive plankton



160 blooms triggered by a physico-chemical phenomenon called Island Mass Effect related to  
161 iron fertilization. In this Cluster, the HgcA sequence OM-RGC.v1.006256245 related to the  
162 *Desulfovibrionales* order (containing most of the experimentally confirmed Hg-methylators)  
163 was the most frequent and abundant in the 23 oxic samples.  
164 The phylogenetic placement of the two sequences grouped in Cluster 2 is poorly supported.  
165 The most abundant sequence was related to *Smithella* and *Desulfomonile tiedjei*  
166 (Syntrophobacterales) while the other one was close to Chloroflexi (Fig. 2, Supplementary  
167 Table 2). HgcA sequences from Cluster 2 were identified in 15 surface and subsurface  
168 samples, mostly in suboxic waters : sequences found in samples with oxygen concentration  
169 below 10  $\mu$ M accounted for 98% of total Cluster 2 abundances (Supplementary Figure 2).  
170 The highest abundances of Cluster 2 HgcA sequences were found in the subsurface waters of  
171 the northern stations within the Arabian Sea Oxygen Minimum Zone (Stations TARA\_036 to  
172 TARA\_039), under the influence of a previous major bloom event, where high particle  
173 concentrations and strong anaerobic microbial respiration have been reported<sup>26</sup>. Cluster 2  
174 sequences were also found in lower abundance in the shallow anoxic zone of the Pacific  
175 North Equatorial Counter Current (Stations TARA\_137 and TARA\_138, see methods).



176

177 **Figure 3 | Distribution of HgcA in Tara Oceans samples**

178 HgcA relative abundance (from 0.01 to 0.1) is indicated by the white-blue gradient. The hierarchical  
 179 clustering highlighted three gene clusters with high abundances in specific samples with marked  
 180 environmental features, as suggested by colored squares. Surface samples were collected in the  
 181 upper layer (< 120 m-depth, in green) while subsurface were collected below 120 m-depth (in grey).  
 182 Seawater was considered as oxic when O<sub>2</sub> > 10 μM (in red) and suboxic when O<sub>2</sub> < 10 μM (in grey).

183 Larger size fraction samples are in dark grey (0.22-3  $\mu\text{m}$ ) and smaller size fractions samples (<0.8  $\mu\text{m}$ )  
184 are in light grey.

185

186

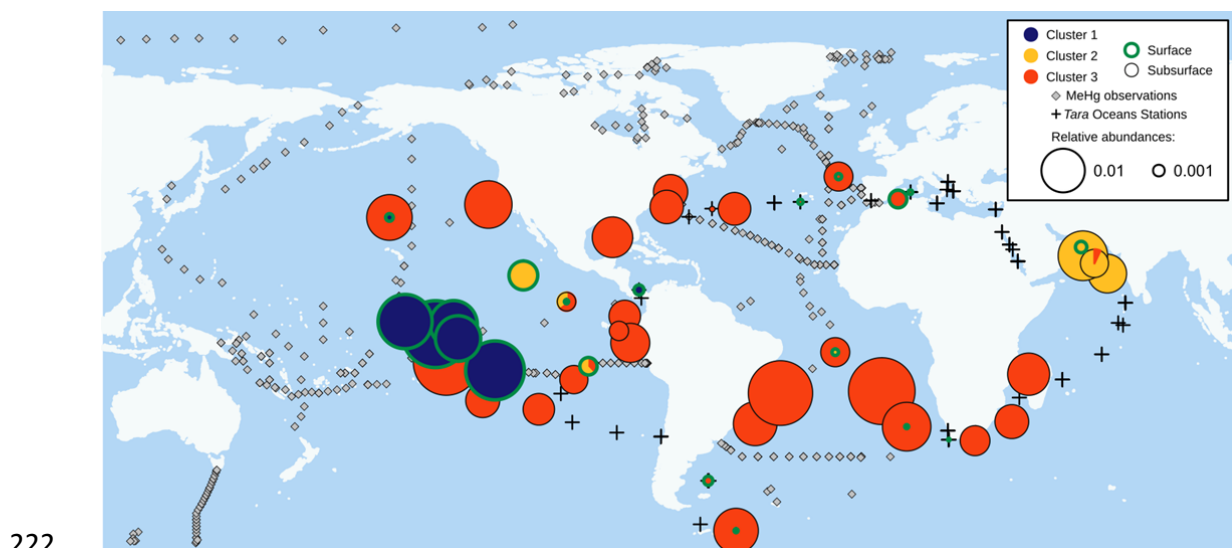
187 The most abundant HgcA-like proteins were grouped in Cluster 3 and were exclusively  
188 assigned to *Nitrospina*. These *Nitrospina* HgcA-like proteins were found in 47 samples,  
189 widespread across all sampled ocean basins. They were almost exclusively found in  
190 subsurface water (> 120 m-depth) and were more frequent in the oxic waters (> 10  $\mu\text{M}_{\text{O}_2}$ ).  
191 Subsurface oxic waters accounted for 84% of total *Nitrospina*-HgcA abundance  
192 (Supplementary Figure 2). Their highest relative abundance was found in the South Atlantic  
193 and the South Pacific Oceans (Fig. 4, Supplementary Table 2). *Nitrospina* HgcA abundance  
194 was positively correlated to nitrate concentration (R 0.54, P < 0.005), which is consistent  
195 with *Nitrospina*'s role as nitrate producer through nitrite oxidation, and with the well-known  
196 nitrate enrichment with depth in the ocean.

197

### 198 ***Nitrospina* as the most predominant and widespread methylator in the open ocean**

199 The predominant and widespread HgcA-like homologs were phylogenetically extremely  
200 close to the *Nitrospina*-related ones (Supplementary Figure 1) previously identified by  
201 metagenomic analysis as potential Hg-methylators within Antarctic sea ice and brine, and  
202 further detected by PCR in seawater samples below the ice<sup>13</sup>. The four *Nitrospina* HgcA-like  
203 sequences from our study were distinct from HgcA in confirmed Hg-methylators, and also  
204 from HgcAB fusion proteins reported in environmental metagenomes<sup>12</sup> (Figure 2). The few  
205 cultured strains harboring a fused *hgcAB* gene (*Methanococcoides methylutens* and  
206 *Pyrococcus furiosus*) were unable to produce MeHg in experimental conditions<sup>12,27</sup>. Through  
207 sequence alignment against Protein Data Bank templates, we confirmed that the four

208 *Nitrospina* HgcA-like homologs showed high conservation of six residue positions involved in  
209 cobalamin binding, which is mandatory for methyl group transfer to Hg<sup>13</sup> (Supplementary  
210 Fig. 1). Protein structure modelling suggests that some *Nitrospina* species may be capable of  
211 Hg-methylation. The observed mutations (N71 and C74) do not suppress Hg methylation  
212 capacity, according to mutagenesis experiments in the model methylator *D. desulfuricans*  
213 ND132<sup>15</sup>. The strictly conserved cysteine facilitates the transfer of methyl groups to  
214 inorganic Hg<sup>28</sup>. The two current *Nitrospina* isolates (*N. gracilis* and *N. watsonii*) have not  
215 been experimentally tested to date for their Hg-methylation capacity. *N. gracilis* genome  
216 lacks the *hgcA* gene. The complete genome of *N. watsonii* is not available. From the 12  
217 *Nitrospina* genome assemblies available on NCBI at the time of writing, we found HgcA-like  
218 proteins (harbouring the six mandatory residues for Hg-methylation) in three strains only:  
219 SCGC AAA288-L16 (single cell whole genome from 770 m-deep ALOHA station, North Pacific  
220 Ocean), AB-629-B06 (single cell whole genome from dark ocean water column) and LS\_NOB  
221 (from a deep-sea sponge holobiont; Supplementary Fig. 1).



#### 223 **Figure 4 | HgcA biogeography**

224 Circle sizes are proportional to the cumulated HgcA homolog genes abundances at each station. The  
225 pie charts indicate the cluster attribution (legend in the chart), and their border color indicates the

226 sampling depth: surface samples (<120 m-depth) in green and subsurface samples (> 120 m-depth) in  
227 grey. *Tara* Oceans stations without detected *HgcAB* genes are represented by black crosses and  
228 seawater MeHg profiles from the literature (Supplementary Text 1) by black diamonds.

229

230 Mercury methylation has long been described for anaerobic environments <sup>12</sup> and *hgcA* genes  
231 have been found exclusively in anaerobic Bacteria and Archea <sup>5</sup>. Yet, we find the most  
232 abundant HgcA homologs are strongly dominant in oxic subsurface samples, where they  
233 coincide with the subsurface MeHg concentration peaks <sup>6</sup>, and are carried by the nitrite  
234 oxidizing bacteria *Nitrospina*, usually considered as aerobic.

235 Several clues may explain this apparent contradiction. First, it is increasingly recognized that  
236 anaerobic processes can occur in anoxic niches such as organic matter aggregates in the  
237 middle of oxic waters <sup>8</sup>. *Nitrospina* sequences were predominantly present in the larger size  
238 fractions (accounting for 78% of total HgcA abundances), suggesting that Hg-methylation -as  
239 other anaerobic processes- might be associated with particles, where anoxic niches are likely  
240 to be favourable to *Nitrospina* methylating activity. Several features suggest the adaptation  
241 of *Nitrospina* to low-oxygen environments. *Nitrospina* have been detected as particularly  
242 abundant (up to 10% of the bacterial community) in several upwelling and oxygen-deficient  
243 zones <sup>29</sup>.

244 Comparative genomics revealed a close evolutionary relationship between *Nitrospina* and  
245 Anammox bacteria, including horizontal gene transfer events, suggesting the coexistence of  
246 these organisms in hypoxic or anoxic environments <sup>16</sup>, as confirmed in incubation  
247 experiments <sup>30,31</sup>. Genome analysis of several *Nitrospina* strains revealed unexpected  
248 adaptation features to low-oxygen environments: no ROS defence mechanism, dependence  
249 on highly oxygen-sensitive enzymes for carbon fixation, and high O<sub>2</sub>-affinity cytochromes  
250 <sup>16,32</sup>.

251 *Nitrospina* can play diverse ecological roles beyond the nitrogen cycle<sup>33</sup>. *Nitrospina* can use  
252 alternative anaerobic pathways to gain energy, using other terminal electron acceptors than  
253 O<sub>2</sub> during fermentation under hypoxic or anaerobic conditions, such as sulfur compounds or  
254 metal oxides. Their capacity to cope with environmental Hg through methylation is worth  
255 considering, since their genome is well equipped against other toxic compounds (arsenate-  
256 and mercuric-reductase, metallic cation transporters, multidrug export system)<sup>16,32</sup>.  
257 Mercury methylation potential might have been acquired by horizontal gene transfer.  
258 Within the four *Nitrospina* scaffolds harbouring *hgcA*, other neighbour genes related to  
259 methyl group transfer and Hg metabolism are found, such as the *merR1* regulator of the *mer*  
260 operon involved in Hg resistance, the *ubiE* methyltransferase and the putative metal-binding  
261 YHS domain (Fig. 1). This genomic context can lead to hypothesize that the expression of  
262 these genes, including *hgcA*, is under the same Hg-induced regulation as the *mer* operon,  
263 triggered by *merR*.  
264 The choice of *hgcAB* as an indicator of Hg-methylation has to be discussed. First, the  
265 presence of *hgcAB* appears necessary but not sufficient for Hg methylation. Indeed,  
266 unsuccessful attempts to transfer Hg-methylation capacity to a non-Hg-methylating strain  
267 suggest that unidentified additional genes might be needed for effective MeHg production  
268<sup>15</sup>. Several critical steps are involved in the Hg-methylation process, such as Hg(II) sensing,  
269 cellular uptake of Hg(II) by active transport, methyl-group providing and transfer, and MeHg  
270 export from the cell. All these steps could be targeted as functional markers of Hg-  
271 methylation in the environment in order to provide a more complete picture of the process.  
272 Second, the exact contribution of *HgcAB* to Hg-methylation is not well understood. Since Hg  
273 methylation does not confer Hg resistance, it cannot be considered as a protection  
274 mechanism against Hg toxicity<sup>19</sup>. In model strains *D. dechloroacetivorans*, net Hg

275 methylation was not clearly induced by inorganic Hg and not significantly correlated to  
276 *hgcAB* gene expression levels, but rather influenced by environmental factors, growth  
277 conditions and energetic metabolism<sup>19,34</sup>. The variability of the methylation potential has  
278 been evidenced in different strains, and the implication of *hgcAB* might also vary between  
279 strains. Such functional gene approaches are powerful to track biogeochemical potentials in  
280 extended environments but remain limited to well described metabolic pathways, ignoring  
281 genes with unknown function<sup>35</sup>.

282 Here, we bring metagenomic evidence for widespread presence of microbial Hg-methylators  
283 in the global ocean, thus reconciling with previous geochemical hints pointing to *in situ*  
284 MeHg production in the water column. The key Hg-methylating genes found across all  
285 oceans corresponded to taxonomic relatives of known Hg-methylators from  
286 Deltaproteobacteria, Firmicutes and Chloroflexi phyla. We further identified the  
287 microaerophilic NOB *Nitrospina* as the potential dominant Hg-methylator in the global  
288 ocean, ubiquitous at the DNA-level, and favoured by oxic subsurface waters (Supplementary  
289 Figure 2). A critical next step would be to examine their *hgcA* expression levels and to  
290 evaluate Hg-methylation capacity in *Nitrospina* cultures. Further studies should also  
291 determine the physicochemical parameters controlling *Nitrospina* Hg-methylation activity  
292 level, in order to better understand how they will respond to expected global changes. Our  
293 results open new avenues for disentangling the functional role of microorganisms in marine  
294 Hg cycling. Our analysis of the *Tara* Oceans metagenomes reveals global distribution of the  
295 key Hg methylating genes (*hgcA* and *hgcB*) and pinpoints *Nitrospina* as responsible for  
296 widespread open ocean MeHg production in subsurface oxic seawater. Our study implicates  
297 the subsurface oxic waters of all oceans as potential source of MeHg that should be  
298 considered in the global Hg-cycle budgets, and identifies microbial target for further



299 research on marine MeHg production. We hypothesize that besides anthropogenic Hg  
300 emissions, ongoing global climate change might have a previously underestimated effect on  
301 *in situ* marine MeHg production by water-column microorganisms, by disturbing microbial  
302 assemblages, activity, and environmental drivers governing Hg-methylation.

303 Methods

#### 304 **Identification of HgcAB environmental sequences in oceanic metagenomes.**

305 *hgcA* and *hgcB* genes encode for a putative corrinoid protein, HgcA, and a [2Fe-4S]  
306 ferredoxin, HgcB, serving respectively as methyl group carrier and electron donor for  
307 corrinoid cofactor reduction. HgcA and HgcB homologs were retrieved by searching Hidden  
308 Markov Model profiles (HMM)<sup>36</sup> provided by Podar et al.<sup>12</sup> in the Ocean Microbial  
309 Reference Gene Catalog<sup>14</sup> (OM-RGC) using the Ocean Gene Atlas<sup>37</sup> ([http://tara-  
310 oceans.mio.osupytheas.fr/ocean-gene-atlas/](http://tara-oceans.mio.osupytheas.fr/ocean-gene-atlas/)). The OM-RGC is the most exhaustive catalogue  
311 of marine genes to date including datasets from *Tara* Oceans metagenomic assemblies and  
312 other publicly available marine genomic and metagenomic datasets. We applied an e-value  
313 threshold of 1e-20. The corresponding scaffolds (i.e. the assembled sequences where the  
314 homolog genes were predicted) were retrieved from the raw assemblies deposited at ENA  
315 (Supp Data 1 & 4). Eight scaffolds without *Tara* Oceans mapped reads were discarded. The  
316 remaining scaffolds were annotated using Prokka with default parameters<sup>38</sup>. The resulting  
317 translated sequences were aligned separately for HgcA and HgcB using Jalview 2.10 and  
318 alignments were cleaned manually<sup>39</sup>. For further analysis, we kept HgcA sequences if they  
319 possess the conserved motif NVWCAA<sup>5</sup>, or if the neighbouring HgcB sequence was present  
320 on the scaffold.

#### 321 **HgcA phylogenetic analysis.**

322 A phylogenetic tree was built from the 10 HgcA sequences kept, 55 HgcA protein sequences  
323 representative of known Hg-methylator clades belonging to Archaea, Firmicutes, Chloroflexi  
324 and Deltaproteobacteria, including 18 experimentally-confirmed Hg-methylators (initially  
325 published by Parks et al.<sup>5</sup>, and updated at  
326 <https://www.esd.ornl.gov/programs/rsfa/data.shtml>), as well as 9 HgcAB fusion proteins<sup>13</sup>  
327 and 3 HgcA-like proteins predicted from *Nitrospina* genome assemblies using Prokka<sup>38</sup>. The  
328 tree was rooted with 3 paralogs from confirmed non-Hg-methylating strains<sup>13</sup>. The closest  
329 sequences (i.e. best e-value match) of each environmental HgcA sequence were retrieved  
330 using BLASTp against non-redundant RefSeq protein database excluding sequences from  
331 uncultured organisms<sup>40</sup>, and included in the tree.

332 The 80 sequences were aligned using MAFFT<sup>41</sup> and gap-containing sites were removed using  
333 the mode gappyout of TrimAl<sup>42</sup>. Maximum likelihood phylogenies were inferred using  
334 PhyML Best AIC Tree (version 1.02b) implemented in Phylemon<sup>43</sup> (version 2.0) with the best  
335 model of sequence evolution Blosum62+I+G+F. Branch support was calculated using the  
336 non-parametric Shimodaira-Hasegawa-like approximate likelihood ratio test. The final tree  
337 was edited using Evolview<sup>44</sup>, especially by annotating the isolation sites retrieved from  
338 Genomes OnLine Database<sup>45</sup>.

### 339 **Conserved sites in HgcA.**

340 Four sequences from OM-RGC related to *Nitrospina* were aligned with the same Protein  
341 Data Bank (PDB) templates as Gionfriddo et al.<sup>13</sup>, as well as the 3 HgcA-like proteins from  
342 *Nitrospina* genome assemblies, and conserved residues were checked. The chosen PDB  
343 structural templates (4djd\_C, 2h9a\_A, 4C1n\_C, 2ycl\_A) were the gamma subunit of the  
344 corrinoid S-Fe acetyl-CoA decarbonylase/synthase complex, identified by Gionfriddo et al.<sup>13</sup>  
345 as the closest and most complete relative to currently unresolved HgcA structure.

346 **Biogeography of HgcA.**

347 Relative HgcA abundances in *Tara* Oceans samples were obtained from the Ocean Gene  
348 Atlas<sup>37</sup>. We screened 243 metagenomes from 68 sites covering the World Ocean except  
349 Arctic, sampled at different depths from surface to 500 m-depth, covering six different size  
350 fractions ranging from 0 to 3  $\mu\text{m}$ . Environmental data were obtained from Pesant et al.<sup>46</sup>  
351 (Supplementary Table 2). For the following analysis, we considered two depths classes  
352 (surface samples < 120 m-depth, subsurface samples > 120 m-depth), two particle size  
353 fractions (< 5  $\mu\text{m}$ , < 0.8  $\mu\text{m}$ ), two oxic states (oxic:  $\text{O}_2 > 10 \mu\text{M}$ , suboxic:  $\text{O}_2 < 10 \mu\text{M}$ ).  
354 HgcA relative abundance was calculated as follows: the length-normalized count of genes  
355 read was divided by the median of the length-normalized counts of a set of ten universal  
356 single copy marker genes<sup>47,48</sup>. Thus, relative abundance represents the fraction of bacteria  
357 harbouring the *hgcA* gene within the assembled genomes. A heatmap of the relative gene  
358 abundances in *Tara* Oceans samples was generated in R<sup>49</sup> using the heatmap.2 function in  
359 the ggplot CRAN library. Dendrograms were computed using hclust default parameters from  
360 Ward distance index based on presence/absence of the genes ('binary' option). Genes were  
361 clustered into three groups (Cluster 1, Cluster 2 and Cluster 3) according to their abundance  
362 pattern on the heatmap. The geographic origin of the *hgcA* genes retrieved from the *Tara*  
363 Oceans samples was plotted on a global map using the "mapplots" R package. At each  
364 station, the cumulated abundance and phylogenetic affiliation of the retrieved *hgcA* genes  
365 were represented on the map by the size and colour of the points. Cluster distribution was  
366 also plotted against depth and oxygen concentration at each station to depict the  
367 environmental conditions where each Cluster flourishes (Supplementary Figure 2). Tracks of  
368 MeHg records from previous campaigns were searched in the literature (Supplementary Text  
369 1) and georeferenced on the map.

370

371 References

- 372 1. Outridge, P. M., Mason, R. P., Wang, F., Guerrero, S. & Heimbürger-Boavida, L. E.  
373 Updated Global and Oceanic Mercury Budgets for the United Nations Global Mercury  
374 Assessment 2018. *Environ. Sci. Technol.* **52**, 11466–11477 (2018).
- 375 2. Gilmour, C. C. *et al.* Mercury methylation by novel microorganisms from new  
376 environments. *Environ. Sci. Technol.* **47**, 11810–11820 (2013).
- 377 3. Gilmour, C. C. *et al.* Sulfate-Reducing Bacterium *Desulfovibrio desulfuricans* ND132 as  
378 a Model for Understanding Bacterial Mercury Methylation. *Appl. Environ. Microbiol.*  
379 **77**, 3938–3951 (2011).
- 380 4. Mason, R. P. *et al.* Mercury biogeochemical cycling in the ocean and policy  
381 implications. *Environ. Res.* **119**, 101–117 (2012).
- 382 5. Parks, J. M. *et al.* The genetic basis for bacterial mercury methylation. *Science (80-. )*.  
383 **339**, 1332–1335 (2013).
- 384 6. Schlitzer, R. *et al.* The GEOTRACES Intermediate Data Product 2017. *Chem. Geol.* **493**,  
385 210–223 (2018).
- 386 7. Ortiz, V. L., Mason, R. P. & Evan Ward, J. An examination of the factors influencing  
387 mercury and methylmercury particulate distributions, methylation and demethylation  
388 rates in laboratory-generated marine snow. *Mar. Chem.* **177**, 753–762 (2015).

- 389 8. Bianchi, D., Weber, T. S., Kiko, R. & Deutsch, C. Global niche of marine anaerobic  
390 metabolisms expanded by particle microenvironments. *Nat. Geosci.* 1–6 (2018).  
391 doi:10.1038/s41561-018-0081-0
- 392 9. Lehnherr, I., St. Louis, V. L., Hintelmann, H. & Kirk, J. L. Methylation of inorganic  
393 mercury in polar marine waters. *Nat. Geosci.* **4**, 298–302 (2011).
- 394 10. Blum, J. D. Marine mercury breakdown. *Nat. Geosci.* **4**, 139–140 (2011).
- 395 11. Masbou, J. *et al.* Carbon Stable Isotope Analysis of Methylmercury Toxin in Biological  
396 Materials by Gas Chromatography Isotope Ratio Mass Spectrometry. *Anal. Chem.* **87**,  
397 11732–11738 (2015).
- 398 12. Podar, M. *et al.* Global prevalence and distribution of genes and microorganisms  
399 involved in mercury methylation. *Sci. Adv.* **1**, (2015).
- 400 13. Gionfriddo, C. M. *et al.* Microbial mercury methylation in Antarctic sea ice. *Nat.*  
401 *Microbiol.* **1**, 16127 (2016).
- 402 14. Sunagawa, S. *et al.* Ocean plankton. Structure and function of the global ocean  
403 microbiome. *Science* **348**, 1261359 (2015).
- 404 15. Smith, S. D. *et al.* Site-directed mutagenesis of HgcA and HgcB reveals amino acid  
405 residues important for mercury methylation. *Appl. Environ. Microbiol.* **81**, 3205–17  
406 (2015).
- 407 16. Lückner, S., Nowka, B., Rattei, T., Spieck, E. & Daims, H. The Genome of *Nitrospina*  
408 *gracilis* Illuminates the Metabolism and Evolution of the Major Marine Nitrite

- 409           Oxidizer. *Front. Microbiol.* **4**, 27 (2013).
- 410    17.    Spieck, E., Keuter, S., Wenzel, T., Bock, E. & Ludwig, W. Characterization of a new  
411           marine nitrite oxidizing bacterium, *Nitrospina watsonii* sp. nov., a member of the  
412           newly proposed phylum “Nitrospinae”. *Syst. Appl. Microbiol.* **37**, 170–176 (2014).
- 413    18.    Cao, J. *et al.* *Pseudodesulfovibrio indicus* gen. nov., sp. nov., a piezophilic sulfate-  
414           reducing bacterium from the Indian Ocean and reclassification of four species of the  
415           genus *Desulfovibrio*. *Int. J. Syst. Evol. Microbiol.* **66**, 3904–3911 (2016).
- 416    19.    Gilmour, C. C. *et al.* Sulfate-reducing bacterium *Desulfovibrio desulfuricans* ND132 as  
417           a model for understanding bacterial mercury methylation. *Appl. Environ. Microbiol.*  
418           **77**, 3938–51 (2011).
- 419    20.    Bae, H.-S., Dierberg, F. E. & Ogram, A. Syntrophs dominate sequences associated with  
420           the mercury methylation-related gene *hgcA* in the water conservation areas of the  
421           Florida Everglades. *Appl. Environ. Microbiol.* **80**, 6517–26 (2014).
- 422    21.    Sorokin, D. Y., Tourova, T. P., Mußmann, M. & Muyzer, G. *Dethiobacter alkaliphilus*  
423           gen. nov. sp. nov., and *Desulfurivibrio alkaliphilus* gen. nov. sp. nov.: two novel  
424           representatives of reductive sulfur cycle from soda lakes. *Extremophiles* **12**, 431–439  
425           (2008).
- 426    22.    Tidjani Alou, M. *et al.* Gut Bacteria Missing in Severe Acute Malnutrition, Can We  
427           Identify Potential Probiotics by Culturomics? *Front. Microbiol.* **8**, 899 (2017).
- 428    23.    Regnell, O. & Watras, C. J. Microbial Mercury Methylation in Aquatic Environments: A

- 429            Critical Review of Published Field and Laboratory Studies. *Environ. Sci. Technol.* **53**, 4–  
430            19 (2019).
- 431    24.    Sela-Adler, M. *et al.* Co-existence of Methanogenesis and Sulfate Reduction with  
432            Common Substrates in Sulfate-Rich Estuarine Sediments. *Front. Microbiol.* **8**, 766  
433            (2017).
- 434    25.    Pak, K. R. & Bartha, R. Mercury methylation by interspecies hydrogen and acetate  
435            transfer between sulfidogens and methanogens. *Appl. Environ. Microbiol.* **64**, 1987–  
436            1990 (1998).
- 437    26.    Roullier, F. *et al.* Particle size distribution and estimated carbon flux across the  
438            Arabian Sea oxygen minimum zone. *Biogeosciences* **11**, 4541–4557 (2014).
- 439    27.    Gilmour, C. C., Bullock, A. L., McBurney, A., Podar, M. & Elias, D. A. Robust mercury  
440            methylation across diverse methanogenic Archaea. *MBio* **9**, (2018).
- 441    28.    Zhou, J., Riccardi, D., Beste, A., Smith, J. C. & Parks, J. M. Mercury Methylation by  
442            HgcA: Theory Supports Carbanion Transfer to Hg(II). *Inorg. Chem.* **53**, 772–777 (2014).
- 443    29.    Levipan, H. A., Molina, V. & Fernandez, C. Nitrospina-like bacteria are the main drivers  
444            of nitrite oxidation in the seasonal upwelling area of the Eastern South Pacific (Central  
445            Chile ~36°S). *Environ. Microbiol. Rep.* **6**, 565–573 (2014).
- 446    30.    Füssel, J. *et al.* Nitrite oxidation in the Namibian oxygen minimum zone. *ISME J.* **6**,  
447            1200–1209 (2012).
- 448    31.    Beman, J. M., Leilei Shih, J. & Popp, B. N. Nitrite oxidation in the upper water column



- 449 and oxygen minimum zone of the eastern tropical North Pacific Ocean. *ISME J.* **7**,  
450 2192–2205 (2013).
- 451 32. Ngugi, D. K., Blom, J., Stepanauskas, R. & Stingl, U. Diversification and niche  
452 adaptations of Nitrospina-like bacteria in the polyextreme interfaces of Red Sea  
453 brines. *ISME J.* **10**, 1383–1399 (2016).
- 454 33. Daims, H., Lückner, S. & Wagner, M. A New Perspective on Microbes Formerly Known  
455 as Nitrite-Oxidizing Bacteria. *Trends Microbiol.* **24**, 699–712 (2016).
- 456 34. Goñi-Urriza, M. *et al.* Relationships between bacterial energetic metabolism, mercury  
457 methylation potential, and *hgcA/hgcB* gene expression in *Desulfovibrio*  
458 *dechloroacetivorans* BerOc1. *Environ. Sci. Pollut. Res.* **22**, 13764–13771 (2015).
- 459 35. Reed, D. C., Algar, C. K., Huber, J. A. & Dick, G. J. Gene-centric approach to integrating  
460 environmental genomics and biogeochemical models. *Proc. Natl. Acad. Sci. U. S. A.*  
461 **111**, 1879–84 (2014).
- 462 36. Eddy, S. R. Accelerated profile HMM searches. *PLoS Comput. Biol.* **7**, e1002195 (2011).
- 463 37. Villar, E. *et al.* The Ocean Gene Atlas: exploring the biogeography of plankton genes  
464 online. *Nucleic Acids Res.* **46**, W289–W295 (2018).
- 465 38. Seemann, T. Prokka: rapid prokaryotic genome annotation. *Bioinformatics* **30**, 2068–  
466 2069 (2014).
- 467 39. Waterhouse, A. M., Procter, J. B., Martin, D. M. A., Clamp, M. & Barton, G. J. Jalview  
468 Version 2—a multiple sequence alignment editor and analysis workbench.

- 469            *Bioinformatics* **25**, 1189–1191 (2009).
- 470    40.    Altschul, S. F., Gish, W., Miller, W., Myers, E. W. & Lipman, D. J. Basic local alignment  
471            search tool. *J. Mol. Biol.* **215**, 403–410 (1990).
- 472    41.    Katoh, K. & Standley, D. M. MAFFT multiple sequence alignment software version 7:  
473            improvements in performance and usability. *Mol. Biol. Evol.* **30**, 772–780 (2013).
- 474    42.    Capella-Gutierrez, S., Silla-Martinez, J. M. & Gabaldon, T. trimAl: a tool for automated  
475            alignment trimming in large-scale phylogenetic analyses. *Bioinformatics* **25**, 1972–  
476            1973 (2009).
- 477    43.    Sanchez, R. *et al.* Phylemon 2.0: a suite of web-tools for molecular evolution,  
478            phylogenetics, phylogenomics and hypotheses testing. *Nucleic Acids Res.* **39**, W470–  
479            W474 (2011).
- 480    44.    Gao, S. *et al.* Evolveview v2: an online visualization and management tool for  
481            customized and annotated phylogenetic trees. *Nucleic Acids Res.* **44**, W236–W241  
482            (2016).
- 483    45.    Mukherjee, S. *et al.* Genomes OnLine Database (GOLD) v.6: data updates and feature  
484            enhancements. *Nucleic Acids Res.* **45**, D446–D456 (2017).
- 485    46.    Pesant, S. *et al.* Open science resources for the discovery and analysis of Tara Oceans  
486            data. *Sci. Data* **2**, 150023 (2015).
- 487    47.    Mende, D. R., Sunagawa, S., Zeller, G. & Bork, P. Accurate and universal delineation of  
488            prokaryotic species. *Nat. Methods* **10**, 881–884 (2013).

489 48. Sunagawa, S. *et al.* Metagenomic species profiling using universal phylogenetic  
490 marker genes. *Nat. Methods* **10**, 1196–1199 (2013).

491 49. R Development Core Team. R: A Language and Environment for Statistical Computing.  
492 (2008).

493

494

#### 495 **Acknowledgements**

496 The authors thank Patricia Bonin, Joana R.H. Boavida, Pascal Hingamp, Eric Pelletier, Daniel  
497 Cossa, Jeroen E. Sonke for constructive comments that helped to improve this manuscript.

#### 498 **Funding**

499 E.V. received funding from the project IMPEKAB ANR-15-CE02-0011

#### 500 **Author contributions**

501 E.V., L.C. and L.E.H.B. wrote the manuscript. E.V. performed the bioinformatic analyses with  
502 the scientific support of L.C.

503

504